Original Article

Journal of Drought and Climate change Research (JDCR)

Winter 2026, Vol. 4, No. 12, pp 45-72

10.22077/jdcr.2025.9730.1155

Estimation of Spatial-Temporal Variations of Water Quality Parameters Using Remote Sensing: A Case of Mindu Reservoir, Morogoro, Tanzania

Now Leonard Mwampamba[1*], Fue Kadeghe Goodluck[2], Hieronimo Proches[3], Mahoo Henry Fatael[4]

1- Irrigation Engineering and Management, Sokoine University of Agriculture (SUA), Morogoro, Tanzania.
2- Cybernetics and Precision Agriculture, Electronics and Precision Agriculture Lab (EPAL), Sokoine University of Agriculture, Morogoro, Tanzania.
3- Department of Agricultural Engineering, School of Engineering and Technology, Sokoine University of Agriculture, Morogoro, Tanzania.
4- Department of Civil and Water Resources Engineering, School of Engineering and Technology, Sokoine University of Agriculture, Morogoro, Tanzania.
*** corresponding author: nowmwampamba@gmail.com**

Keywords:
Remote Sensing, Water Quality Parameters (WQPs), Turbidity, Total Suspended Solids (TSS), Electrical Conductivity (EC) and potential of Hydrogen (pH)

Received:
12 Jul 2025

Revised:
09 Aug 2025

Accepted:
10 Aug 2025

ABSTRACT

Water quality assessment offers an evidence necessary for making sound decisions toward compliance of water to its designated use. This study used Remote sensing-based algorithms to assess spatial-temporal variations of water quality at Mindu Reservoir in the Morogoro Region for the period of six months from November-2024 to April-2025. Whereby, remotely sensed data were obtained through Sentinel-2 MSI sensor on a satellite temporal resolution basis, and the in-situ data were collected within the same period in the days coinciding and/or closely coinciding (±1 day) with Sentinel-2 satellite visit for better accuracy assessment. The assessed water quality parameters were Turbidity, Total Suspended Solids (TSS), Electrical Conductivity (EC), and potential of Hydrogen (pH). Various algorithms derived from literatures were used in the GEE JavaScript API for mapping water quality parameters (WQPs), and the Microsoft Excel was used to establish regression relationships between the remotely sensed indices and the in-situ measured values. The results show good accuracy and are statistically significant with R^2 =0.7214, ($p<0.00187$); R^2=0.8046, ($p<0.015$); R^2=0.6838, ($p<0.00317$); and R^2=0.7394, ($p<0.0014$) observed in developed algorithms for Turbidity, TSS, EC, and pH estimation respectively. The RMSE and MAE were also used to assess the accuracy of generated algorithms in prediction of the actual in-situ measured data. Highlighting the potentiality of Remote Sensing in retrieving WQPs

How to cite this article:
Mwampamba, N.L., Goodluck, F.K. Proches, H. & Fatael, M.H. (2026). Estimation of Spatial-Temporal Variations of Water Quality Parameters Using Remote Sensing: A Case of Mindu Reservoir, Morogoro, Tanzania. *Journal of Drought and Climate change Research* (JDCR), 4(12), 45-72. https://doi.org.ir/10.22077/jdcr.2025.9730.1155

Introduction

Water quality assessment refers to the overall process of evaluation of the physical, chemical, biological and aesthetic attributes of water in relation to natural quality, human effects and intended uses, including agricultural, domestic, and industrial uses (Chapman, 2021). Water quality is totally linked with water quantity as both are key determiners of supply and that, polluted water that cannot be used for drinking, bathing, industry, and/or agriculture may largely reduce amount of water available for use in a given area, unless some additional costs are incurred to treat/purify water for meeting the desired quality (Eslamian, 2016). The Earth is composed of 70% water, with 3% of fresh water and only 0.06% available without problems. Yet, the demand for water is continuing to increase not only by growing world population but also by its aspirations for an ever increasing standard of living (Koncagül et al., 2020). This demand is rising from irrigation (70%of all water uses), industrial (20%), and domestic (10%); hence, according to United Nations 2.7 billion people (two-thirds of all nations) will not have clean water by 2025 (Chidiac et al., 2023; Ahuja, 2021). With the most serious of all environmental concerns of lack of adequate water of good quality happening in the developing countries (Biswas et al., 2025; Markandya, 2006).

Annual population growth rate of 3.2% (population census, 2022), the increasing pressures from urbanization, agricultural activities increasing at a rate of 4.4%, and climate change in Tanzania, has intensified the extent of placing the water resources at a serious ecological risk (Pauw et al., 2011; Machiwa, 2003). The water resources are decreasing, overused, and degraded threatening the surrounding environment and human life (Al Yousif and Chabuk, 2023).

Water quality at Mindu Reservoir suffers degradation from natural causes and changes in land use land cover; it has been researched that the built-up and cultivated land in the Mindu dam catchment have increased for 61.3% and 72.2% respectively from the year 1990 to 2020 (Gobry, 2023). This increases agricultural runoffs that leads to downstream sedimentation and water quality degradation in the Mindu Reservoir. Despite the huge importance of Mindu Reservoir (dependable source of fresh water supply in Morogoro urban and peri-urban areas), there are limited assessments on the Spatial and Temporal variations of water quality across Mindu Reservoir. The sixth Sustainable Development

Goal (SDG-6), highlights the need for protection, restoration, and sustainable management of water-related ecosystems.

A study by (Ngonyani et al., 2007), assessed Water quality of the Mindu Reservoir based on in-situ measurement, however this approach is proven to be to be expensive, time consuming, and does not provide overall patterns of surface water quality, it rather provides individual concentration of water quality parameter in discrete point format which are difficult for decision-makers to understand (Kc et al., 2019). Alternatively, Remote sensing provides better information due to synoptic spatial and temporal coverage of large areas, accessibility to remote and inaccessible areas, and access to historical data (Govedarica and Jakovljević, 2019). However, Remote sensing based water quality assessment is conducted by directly relating the remote sensing reflectance with in-situ measurements and that, in-situ measurement cannot be replaced in validation and testing of remote sensing (World Water Quality Alliance, 2021; Govedarica and Jakovljević, 2019). Remotely sensed data of Sentinel-2 satellite have a spatial resolution of 10m for its visible and near-infrared bands, which is higher than 30m of Landsat-8 and 500m of MODIS. This allows Sentinel-2 to detect more minor features and provide detailed information important for monitoring smaller water bodies. The Temporal resolution of 5 days of Sentinel-2 can offer near-real-time data that facilitates continuous monitoring of water quality parameters enhancing researchers' and decision makers' ability to monitor water bodies more timely and effectively, making it ideal and suited for cost-effective assessment of water quality parameters like Turbidity, Salinity, Potential of Hydrogen (pH) and Total Suspended Solids (TSS).

Efforts to utilize remote sensing have been done, as for example, a study by (Kimambo et al., 2019), did a retrospective analysis of Chlorophyll-a and its correlation with climate and hydrological variations in Mindu Dam, but there is a lack of comprehensive studies on Turbidity, TSS, pH, and EC at Mindu Reservoir. Building on this foundation, therefore, this study aims to develop remote sensing-based algorithms by assessing the correlation existing between remote sensing spectral signatures of Sentinel-2 satellite and the in-situ data given in Table 2, collected from November 2024 to April 2025 partly covering dry and wet season for monitoring water Turbidity, TSS, pH, and EC at the Mindu Reservoir. Given that

the temporal resolution of Sentinel-2 Satellite is 5 days which implies a new data availability after every satellite passage (five days), therefore, the developed algorithms cannot provide real-time data between the successive visits of the Sentinel-2 Satellite, they rather provide a new data after every satellite passage (five days). However, this will offer near-real-time analysis and provide a cost-effective tool for water quality management.

Materials and Methods

Description of the Study Area

Mindu Reservoir is located in the Wami-Ruvu basin in the south-west of Morogoro municipality within a latitude of 6°51'00''S to 6°53'00''S and a longitude of 37°36'00''E to 37°37'30''E. it collects water from the Mzinga, Lukulunge, Mugera, and Mlali Tributaries of the Ngerengere River and the Uluguru mountain ranges. Mindu Reservoir is a dependable source of water supply and freshwater fishery in Morogoro urban and peri-urban areas, and has an estimated surface area of 3.8 km². It has a bi-modal rainfall pattern with long rains between March and May and short rains between October and December. the average annual rainfall varies between 600mm to 1800mm, and the average annual temperature of 25.0°C through out the year

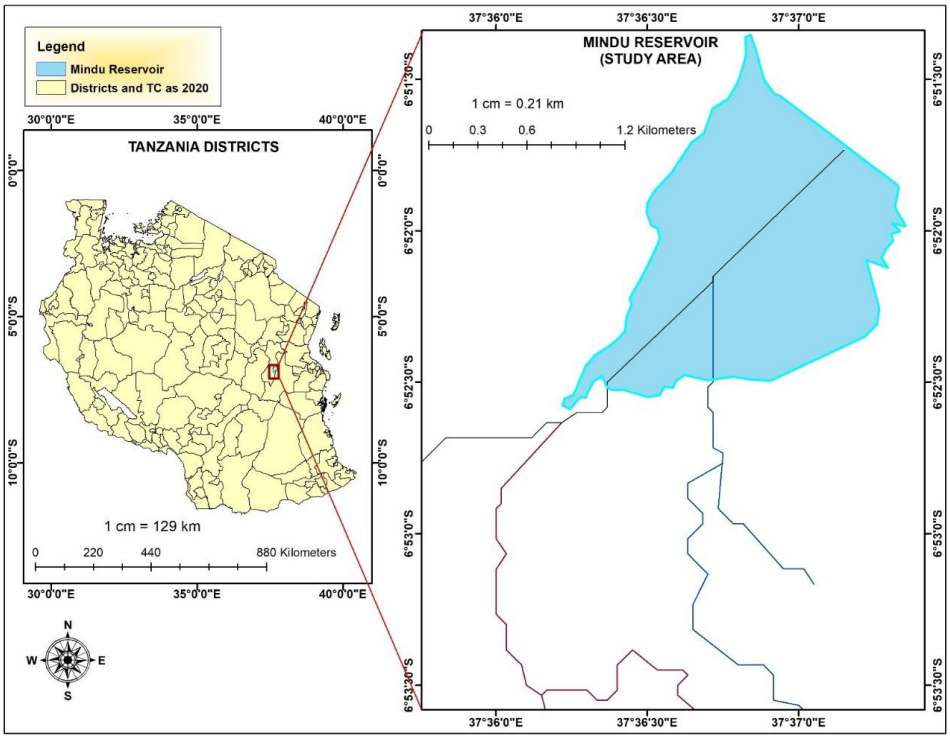

Fig 1. A map showing the location of the study area in Morogoro, Tanzania, developed in ArcGIS version 10.8 environment

Data acquisition and Laboratory Measurements

Field data collection and laboratory analysis was conducted in the Mindu Reservoir and Morogoro Water Laboratory respectively from Nov-2024 to Apr-2025, whereby ten monitoring points were established covering three zones (inlet, mid-section, and outlet) of the Mindu Reservoir (Figure 2), and their water quality monitored in a fortnight interval. the monitored water quality parameters were Turbidity, Electrical Conductivity (EC), potential of Hydrogen (pH), and Total Suspended Solids (TSS); and the rationale for considering 10 sampling points, dividing the reservoir into zones, sampling frequency, and marking the sampling locations was based on the sampling guidelines provided by ISO 5667 which recommends a minimum of 6 samples per year in a 2-month sampling frequency, and allows flexibility depending on a local context (Kapalanga et al., 2021; Sweetnam, 2004; Department of Water Affairs and Forestry, Department of Health, and Water Research Commission, 2000).

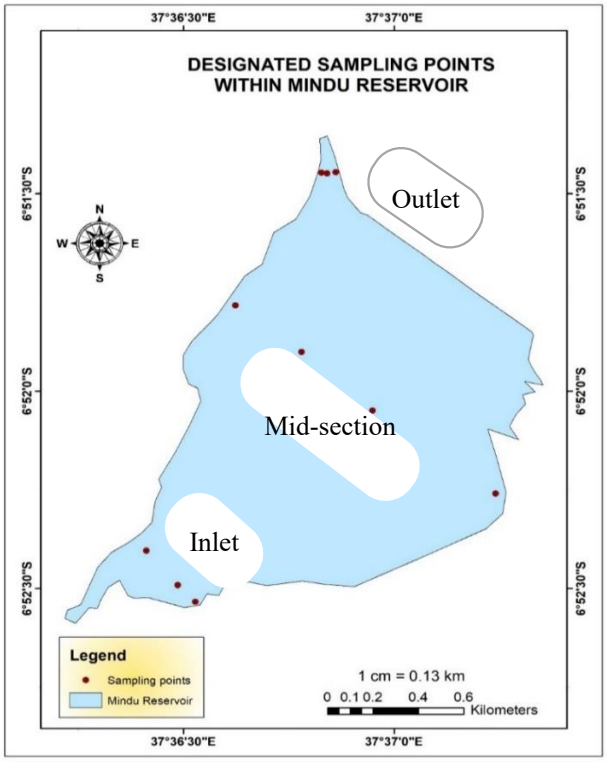

Fig 2. A map showing designated sampling points in the Mindu Reservoir, November-2024 to April-2025

The mean values of the collected data that were coinciding and/or closely coinciding (±1 day) with the days of the satellite (Sentinel-2) visit given in Table 1, were calculated and summarized in Table 2 to ensure better accuracy of the algorithms

Table 1. A table showing days of the sentinel2 satellite visit at Mindu Reservoir

YEAR	2024			2025		
MONTH	Nov	Dec	Jan	Feb	Mar	Apr
DATE OF SENTINEL2 VISIT	5,10,20,25, and 30	5,10, 15, 20, and 30	19	8, 13, 18, 23, and 28	5, 17, 25, and 27	4, 9, 16, 19, and 24

Table 2. Mean values of water parameters collected in the days that were coinciding and/or closely coinciding (±1 day) with the days of the Sentinel-2 visit, Nov-2024 to Apr-2025 at the Mindu Reservoir

Longitude (E)	Latitude (S)	Mean observed-EC	Mean observed-PH	Mean observed-TSS	Mean observed-Turbidity
37.61433°	6.85741°	0.185444	8.0844	36.1111	61.100
37.61408°	6.85745°	0.186556	8.2656	28.8889	52.778
37.61378°	6.85746°	0.184889	8.1278	-	59.211
37.62065°	6.87082°	0.186444	8.5944	-	56.900
37.61632°	6.86770°	0.188111	8.5289	18.8889	50.300
37.61287°	6.86488°	0.185556	8.3611	27.2222	59.478
37.61043°	6.86300°	0.186222	8.3422	-	59.533
37.60667°	6.87332°	0.184	8.2789	-	64.333
37.60808°	6.87494°	0.184333	8.2722	30.0000	59.667
37.60880°	6.87557°	0.184444	8.0567	29.4444	60.222

Analysis and processing of satellite data

The harmonized "[ee. ImageCollection("COPERNICUS/S2_SR_HARMONIZED")]" satellite imagery dataset captured by Sentinel-2 Multispectral Instrument (MSI), level 2A and provided by European Union/ESA/Copernicus has been used in this study. The dataset is available since March-2017 to date and the satellite has revisit interval of 5 days. The L2A satellite set of image (BOA) was obtained from Google Earth Engine (GEE). The GEE data repository and computer algorithms allow cloudless image pixels that approximately coincide with the location and dates of the water quality sampling to be identified (in-situ monitoring locations) Clouds and cirrus filtration function was used in the GEE JavaScript API to process and create free-cloud images over the study site, as clouds are significant barriers to the application of optical remote sensing images and can cause errors in the interpretation of the band reflectance values, and these errors can be transferred to the proposed equations (Barraza-Moraga et al., 2022; Lu, M et al., 2020)

GEE JavaScript API was used to

generate script for image acquisition, processing, band extraction, water layer masking using Modified Normalized Difference Water Index (MNDWI) which uses the Green band (B3) and the Short Wave Infrared1 (SWIR1)-B11 bands of sentinel-2 satellite, calculation of the required water parameter indices, and Generating concentration maps for each water quality parameters (Turbidity, TSS, Salinity and PH).

```
/*.....Creating a Function for Masking clouds.....*/
function maskS2clouds(image) {
  var qa = image.select('QA60');

  // Bits 10 and 11 are clouds and cirrus, respectively.
  var cloudBitMask = 1 << 10;
  var cirrusBitMask = 1 << 11;

  // Both flags should be set to zero, indicating clear conditions.
  var mask = qa.bitwiseAnd(cloudBitMask).eq(0)
      .and(qa.bitwiseAnd(cirrusBitMask).eq(0));

  return image.updateMask(mask).divide(10000)
  .select('B.*').copyProperties(image, ['system:time_start']);
}
```

Fig 3. A section of a GEE–JavaScript for clouds and cirrus filtration in the Mindu Reservoir, November-2024 to April-2025

Table 3. Sentinel-2 bands' specifications

Name	Scale	Pixel Size	Wavelength	Description
B1	0.0001	60 meters	443.9nm (S2A) / 442.3nm (S2B)	Aerosols
B2	0.0001	10 meters	496.6nm (S2A) / 492.1nm (S2B)	Blue
B3	0.0001	10 meters	560nm (S2A) / 559nm (S2B)	Green
B4	0.0001	10 meters	664.5nm (S2A) / 665nm (S2B)	Red
B5	0.0001	20 meters	703.9nm (S2A) / 703.8nm (S2B)	Red Edge 1
B6	0.0001	20 meters	740.2nm (S2A) / 739.1nm (S2B)	Red Edge 2
B7	0.0001	20 meters	782.5nm (S2A) / 779.7nm (S2B)	Red Edge 3
B8	0.0001	10 meters	835.1nm (S2A) / 833nm (S2B)	NIR
B8A	0.0001	20 meters	864.8nm (S2A) / 864nm (S2B)	Red Edge 4
B9	0.0001	60 meters	945nm (S2A) / 943.2nm (S2B)	Water vapor
B10	0.0001	60 meters	1373.5nm (S2A) / 1376.9nm (S2B)	Cirrus
B11	0.0001	20 meters	1613.7nm (S2A) / 1610.4nm (S2B)	SWIR 1
B12	0.0001	20 meters	2202.4nm (S2A) / 2185.7nm (S2B)	SWIR 2

Assessing the relationship existing between in-situ and reflectance values of satellite data

Band combinations necessary for calculating indices of water quality parameters were established from literatures. Where by an index for water Turbidity is found by using the Normalized Difference Turbidity Index (NDTI) which is given by the combination of the red band (B4) and the green band (B3) of sentinel-2 satellite

$$NDTI = \frac{B4 - B3}{B4 + B3}$$

(Das et al., 2024;

Dogliotti et al., 2015)

The NDTI was calculated in the GEE JavaScript API. The reflectance values from sampled locations was then extracted and compared with the in-situ data of the monitored sampling sites, which facilitated the development of an algorithm that describe the mathematical relationship between in-situ Turbidity values and the satellite derived index (NDTI)

```
  //..............Creating a function for calculating NDTI.................
  var NDTI_f = function (img){
  var NDTI =img.normalizedDifference(['B4','B3'])
        .rename ('NDTI');
       return img.addBands(NDTI);};

var NDTI_regression = function (img) {
  var Turbidity_NTU = img.expression(
    '(98.158*x + 71.283)', {
      'x': img.select('NDTI')
    }
  ).rename('Turbidity_NTU');
  return img.addBands(Turbidity_NTU);
};

// Apply the regression function
var NDTI_IMG = NDTI_f(IMG_water);
var Turbidity = NDTI_regression(NDTI_IMG);

// Visualization parameters for Turbidity
var vizNDTI = {
  min: 48.13307847472442,
  max: 74.16825973837305,
  palette: ['blue', 'green', 'yellow', 'orange', 'red']
};

// Add the layer to the map
Map.addLayer(Turbidity.select('Turbidity_NTU'), vizNDTI, 'Turbidity');
```

Fig 4. A section of a GEE–JavaScript for Turbidity estimation in the Mindu Reservoir, November-2024 to April-2025

An index for the Total Suspended Solids (TSS) is calculated using Normalized Difference Suspended Sediment Index (NDSSI) used for mapping Suspended Sediment Concentration (SSC) or Total Suspended Solids which is given by the combination of the Near Infrared band (B8) and the blue band (B2) of sentinel-2 satellite

$$NDSSI = \frac{B8 - B2}{B8 + B2}$$

(Sankaran et al., 2023)

The NDSSI was calculated in the GEE JavaScript API. The reflectance values from sampled locations were then extracted and compared with the in-situ data of the monitored sampling sites, which facilitated the development of an algorithm that describe the mathematical relationship between in-situ TSS values and the satellite derived index (NDSSI)

An Index for water pH is calculated by a combination of Aerosols Band (B1), green band (B3), Red edge2 (B6), and Near Infrared Band (B8) of Sentinel-2 satellite given by “B1 + B3 + B6 + B8”

```
  //..............Creating a function for calculating TSS.............
  var TSS_f = function (img){
   var TSS =img.normalizedDifference(['B8','B2'])
             .rename('TSS');
   return img.addBands(TSS)};

var TSS_regression = function (img) {
  var TSS_mg_per_l = img.expression(
    '(35.751*x + 29.899)', {
      'x': img.select('TSS'),
    }
  ).rename('TSS_mg_per_l');
  return img.addBands(TSS_mg_per_l);
};

// Apply the regression function
var TSS_IMG = TSS_f(IMG_water);
var TSS_LAYER = TSS_regression(TSS_IMG);

// Visualization parameters for Turbidity
var vizTSS = {
  min: 17.577419525519407,
  max:55.68461206542051,
  palette: ['green','yellow','orange', 'red']
};

// Add the layer to the map
Map.addLayer(TSS_LAYER.select('TSS_mg_per_l'), vizTSS, 'TSS');
```

Fig 5. A section of a GEE–JavaScript for TSS estimation in the Mindu Reservoir, November-2024 to April-2025

where by the associated coefficients are found through regression equation (Pizani et al., 2020)

An Index for water pH was calculated in the GEE JavaScript API. The reflectance values from sampled locations were then extracted and compared with the in-situ data of the monitored sampling sites, which facilitated the development of an algorithm that describe the mathematical relationship between in-situ water pH values and the satellite derived index for water pH

```
  //..............Creating a function for calculating PH.............
  var PH_f = function (img){
  var PH = img.expression('B1 + B3 + B6 + B8', {
    'B1': img.select('B1'),
    'B3': img.select('B3'),
    'B6': img.select('B6'),
    'B8': img.select('B8'),
  }).rename('PH');
  return img.addBands(PH);
};
   //Creating PH regression function
   var PH_regression = function (img){
  var PH_value = img.expression('-6.0348*x + 9.5507', {
    'x': img.select('PH'),
    }).rename('PH_value');
  return img.addBands(PH_value);
   };

// Updated visualization parameters to match the actual pH range in your data
var vizPH = {min: 7.91822689311724, max: 8.649892161385957, palette: ['green','cyan','red']};
var PH_IMG = PH_f(IMG_water);
var PH_predict = PH_regression(PH_IMG);

Map.addLayer(PH_predict.select('PH_value'), vizPH, 'PH');
```

Fig 6. A section of a GEE–JavaScript for pH estimation in the Mindu Reservoir, November-2024 to April-2025

An Index for water EC is calculated by a combination of Aerosols Band (B1), blue band (B2), green band (B3), and Near Infrared Band (B8) of Sentinel-2 satellite given by "B1 + B2 + B3 + B8" where by the associated coefficients are found through regression equation (dos Santos, 2022; Pizani et al., 2020) An Index for water EC was calculated in the GEE JavaScript API. The reflectance values from sampled locations were then extracted and compared with the in-situ data of the monitored sampling sites, which facilitated the development of an algorithm that describe the mathematical relationship between in-situ water EC values and the satellite derived index for water EC

```
//..............Creating a function for calculating EC.................
  var EC_f = function (img){
 var EC =img.expression ('B1 + B2 + B3 + B8',{
  'B1':img.select('B1'),
  'B2':img.select('B2'),
  'B3':img.select('B3'),
  'B8':img.select('B8'),
 }).rename('EC');
 return img.addBands(EC)};

var EC_regression = function (img){
var EC_mS_per_cm =img.expression('( -0.0165*x + 0.1896)', {
  'x': img.select('EC'),
}
).rename('EC_mS_per_cm');
return img.addBands(EC_mS_per_cm);
};

//.......adding visualization, mapping the fuction and adding a layer to the map........
var vizEC = {min:0.17669030535601077, max:0.18656992461226882, palette: ['green','purple','orange','red']};
 var EC_IMG = EC_f (IMG_water);
 var EC_Layer = EC_regression (EC_IMG);
 Map.addLayer(EC_Layer.select('EC_mS_per_cm'), vizEC, 'EC_Layer');
```

Fig 7. A section of a GEE–JavaScript for EC estimation in the Mindu Reservoir, November-2024 toApril-2025

The Micro soft excel was used to create regression models for estimating specific parameter's concentration regarding the existing correlation between in-situ measured concentrations versus reflectance values observed in satellite images

Accuracy assessment

The coefficient of determination (R^2) which is referred to as a number that tells how well the independent variable in the statistical model explains variation in the dependent variable was established for each generated algorithm.

$R^2 = \left\{1 - \frac{SSR}{SST}\right\}$,where: SSR is the sum of squared residuals and SST is the total sum of squares

Accuracy assessment was done by comparing the collected in-situ data with the derived remote sensing algorithm data by statistical analysis particularly Root Mean Square Error (RMSE) and Mean Absolute Error (MAE) (Zhang et al., 2023; Barraza-Moraga *et al.,* 2022)

$$RMSE = \sqrt{\frac{1}{n}\sum_{i=1}^{n}(P_i - M_i)^2} \quad (1)$$

$$MAE = \frac{1}{n}\sum_{i=1}^{n} | P_i - M_i \quad (2)$$

Where: 'n' is the number of datasets, subscript 'i' is a single data point

M_i - mean in-situ observed values of concentration of a water quality parameter from Nov 2024 to April 2025

P_i - Predicted (remote sensing-based) mean values of concentration of a water quality parameter within the period of study

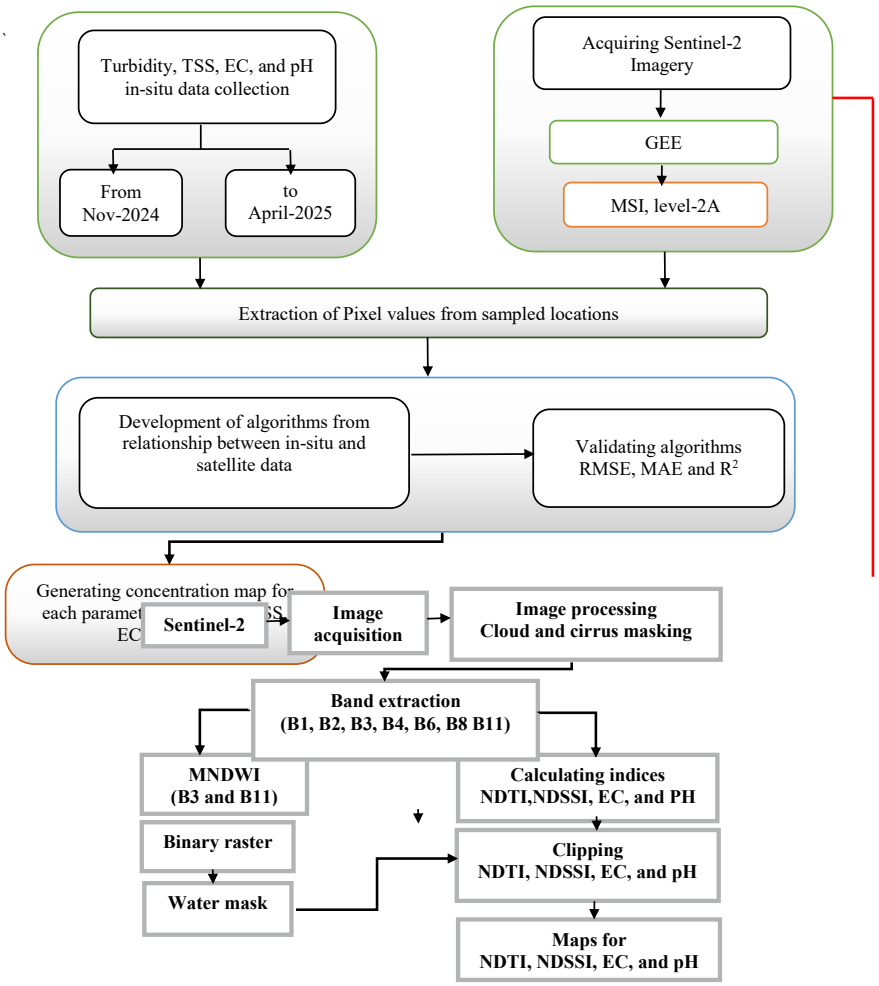

Fig 8. Graphical methodology of the study

Results and Disscussion

Assessing the relationship between in-situ and reflectance values of satellite data

a) Turbidity

The created algorithm showing the correlation between in-situ water Turbidity and the reflectance values observed in satellite images over Mindu Reservoir from Nov 2024 to April 2025 follows a strong linear relationship with the Coefficient of Determination (R^2) value of 0.7214 as

given in equation (3) below

$$Y=98.158x + 71.283 \quad (3)$$

Where; Y- represents Turbidity values in NTU

And X- represents the reflectance values observed in satellite images given by $\frac{B4 - B3}{B4 + B3}$

With: B4-red band of Sentinel-2 (S2A) satellite whose wavelength is 664.5nm and B3- green band of Sentinel-2 (S2A) satellite whose wavelength is 560.0nm

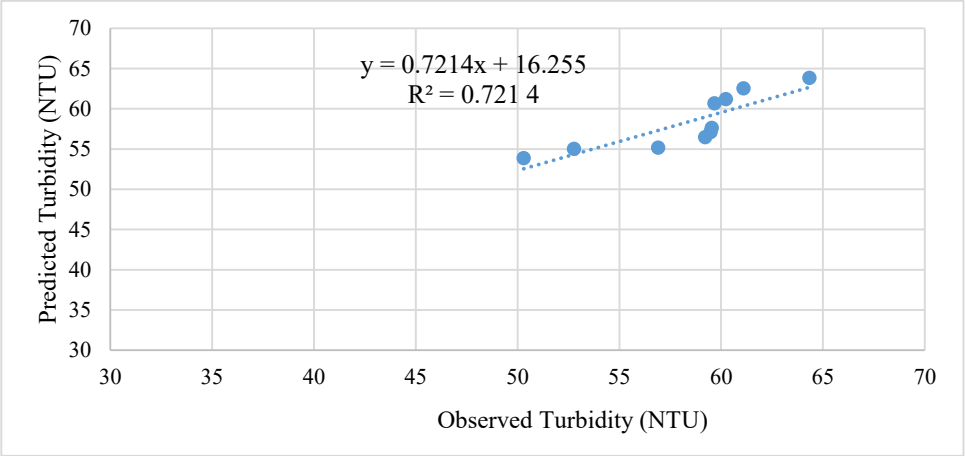

Fig 9. A scatter plot showing the linear relationship between observed and predicted Turbidity (NTU) at Mindu Reservoir, November 2024–April 2025, with $R^2 = 0.7214$.

Table 4. A table of Mean observed and predicted values of water Turbidity in the sampled locations

Pixel	Longitude (E)	Latitude (S)	In-situ measurement (M_i)-Turbidity (NTU)	Predicted (P_i)-Turbidity (NTU)	RMSE	MAE
1	37.61433°	6.85741°	61.100	62.5402	2.0440	1.8450
2	37.61408°	6.85745°	52.778	55.0042		
3	37.61378°	6.85746°	59.211	56.4643		
4	37.62065°	6.87082°	56.900	55.1730		
5	37.61632°	6.86770°	50.300	53.8791		
6	37.61287°	6.86488°	59.478	57.1099		
7	37.61043°	6.86300°	59.533	57.6344		
8	37.60667°	6.87332°	64.333	63.8513		
9	37.60808°	6.87494°	59.667	60.6839		
10	37.60880°	6.87557°	60.222	61.1860		

The regression analysis as shown in Table 5 below, between the observed and predicted Turbidity (NTU) demonstrates a p-value of 0.00187 which is lower than the critical value of 0.05, meaning that the results are statistically significant and there is only 0.187% that the observed correlation between the observed and predicted Turbidity (NTU) is due to chance (Field, 2024). Therefore, the null hypothesis stating "**there is no correlation between observed and predicted Turbidity (NTU) values**" is rejected.

Table 5. A table of regression analysis for Turbidity (NTU) concentration

ANOVA					
	df	SS	MS	F	p-value
Turbidity Regression	1	78.05412	78.05412	20.71855	0.001870037
Residual Error	8	30.13884	3.767355		
Total Turbidity Variation	9	108.193			

b) Total Suspended Solids

The created algorithm showing the correlation between in-situ water TSS and the reflectance values observed in satellite images over Mindu Reservoir from Nov 2024 to April 2025 follows a strong linear relationship with the Coefficient of Determination (R^2) value of 0.8046 as given in equation (4) below

$$Y = 35.751*x + 29.899 \quad (4)$$

Where; Y- represents TSS values in mg/l

And X- represents the reflectance values observed in satellite images given by $\frac{B8 - B2}{B8 + B2}$ which is the formula for Normalized Difference Suspended Sediment Index (NDSSI) used for mapping Suspended Sediment Concentration (SSC) or Total Suspended Solids (Sankaran et al., 2023)

With B8- Near Infrared Band (NIR) of Sentinel-2 satellite (S2A), whose wavelength is 835.1nm, and B2- Blue Band of Sentinel-2 satellite (S2A), whose wavelength is 496.6nm.

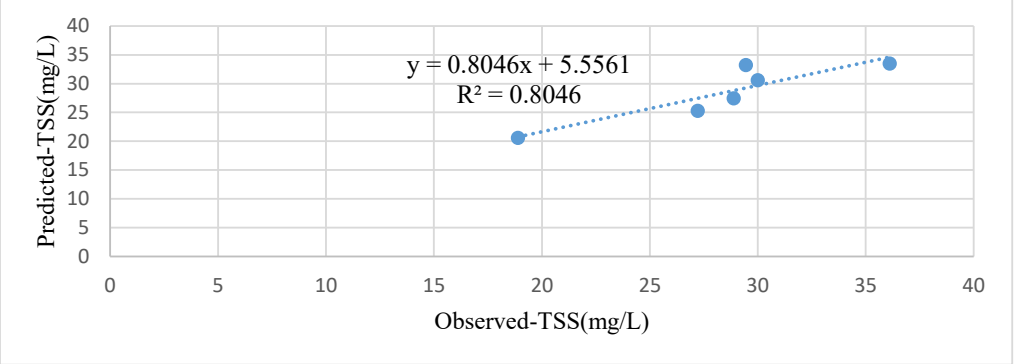

Fig 10. A scatter plot showing the linear relationship between observed and predicted TSS(mg/L) at Mindu Reservoir, November 2024–April 2025, with R^2 = 0.8046.

Table 6. A table of Mean observed and predicted values of water TSS in the sampled locations

Pixel	Longitude (E)	Latitude (S)	In-situ measurement (M_i)-TSS ($\frac{mg}{L}$)	Predicted (P_i)-TSS ($\frac{mg}{L}$)	RMSE	MAE
1	37.61433°	6.85741°	36.1111	33.4603		
2	37.61408°	6.85745°	28.8889	27.4562		
3	37.61632°	6.86770°	18.8889	20.6075	2.2484	2.0160
4	37.61287°	6.86488°	27.2222	25.2585		
5	37.60808°	6.87494°	30.0000	30.5734		
6	37.60880°	6.87557°	29.4444	33.2014		

The regression analysis as shown in Table 7 below, between the observed and predicted TSS (mg/L) demonstrates a p-value of 0.015 which is lower than the critical value of 0.05, meaning that the results are statistically significant and there is only 1.5% that the observed correlation between the observed and predicted TSS (mg/L) is due to chance. Therefore, the null hypothesis stating "**there is no correlation between observed and predicted TSS (mg/L) values**" is rejected.

Table 7. A table of regression analysis for TSS (mg/L) concentration

ANOVA					
	df	SS	MS	F	p-value
TSS Regression	1	100.4589	100.4589	16.46613	0.015375933
Residual Error	4	24.40376	6.100941		
Total TSS Variation	5	124.8627			

c) Water pH

The created algorithm showing the correlation between in-situ water pH and the reflectance values observed in satellite images over Mindu Reservoir from Nov 2024 to April 2025 follows a strong linear relationship with the Coefficient of Determination (R^2) value of 0.7394 as given in equation (5) below

$$Y = -6.0348x + 9.5507 \quad (5)$$

Where; Y- represents water pH values

And X- represents the reflectance values observed in satellite images given by B1 + B3 + B6 + B8 combining bands of sentinel-2 satellite namely B1, B3, B6 and B8 where by the associated coefficients are found through regression equation (Pizani et al., 2020)

With B1- Aerosols Band of Sentinel-2 (S2A) satellite whose wavelength is 443.9nm,

B3- green band of Sentinel-2 (S2A) satellite whose wavelength is 560nm,

B6- Red edge2 band of Sentinel-2 (S2A) satellite whose wavelength is 740.2nm,

B8- Near Infrared Band (NIR) of Sentinel-2 (S2A) satellite whose wavelength is 835.1nm,

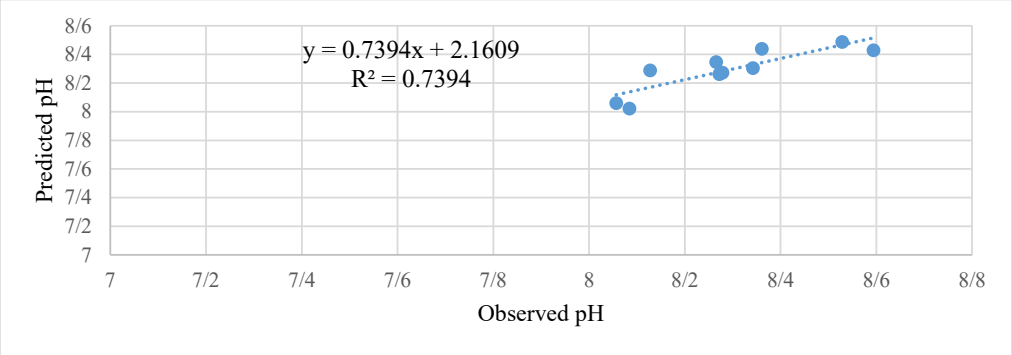

Fig 11. A scatter plot showing the linear relationship between observed and predicted water-pH at Mindu Reservoir, November 2024–April 2025, with $R^2 = 0.7394$.

Table 8. A table of Mean observed and predicted values of water pH in the sampled locations

Pixel	Longitude (E)	Latitude (S)	In-situ measurement (M_i)- pH	Predicted (P_i)- pH	RMSE	MAE
1	37.61433°	6.85741°	8.0844	8.0224		
2	37.61408°	6.85745°	8.2656	8.3459		
3	37.61378°	6.85746°	8.1278	8.2894		
4	37.62065°	6.87082°	8.5944	8.4282		
5	37.61632°	6.86770°	8.5289	8.4862	0.0857	0.0647
6	37.61287°	6.86488°	8.3611	8.4385		
7	37.61043°	6.86300°	8.3422	8.3051		
8	37.60667°	6.87332°	8.2789	8.2728		
9	37.60808°	6.87494°	8.2722	8.2629		
10	37.60880°	6.87557°	8.0567	8.0607		

The regression analysis as shown in Table 9 below, between the observed and predicted water pH demonstrates a p-value of 0.0014 which is lower than the critical value of 0.05, meaning that the results are statistically significant and there is only 0.14% that the observed correlation between the observed and predicted water pH is due to chance. Therefore, the null hypothesis stating "**there is no correlation between observed and predicted water pH values**" is rejected.

Table 9. A table of regression analysis for water pH concentration

ANOVA					
	df	SS	MS	F	p-value
water pH Regression	1	0.153929824	0.15392982	22.69499	0.00141963
Residual Error	8	0.054260374	0.00678255		
Total water pH Variation	9	0.208190198			

d) Water EC

The created algorithm showing the correlation between in-situ water Electrical Conductivity and the reflectance values observed in satellite images over Mindu Reservoir from Nov 2024 to April 2025 follows a strong linear relationship with the Coefficient of Determination (R^2) value of 0.6838 as given in equation (6) below

$$Y = -0.0165x + 0.1896 \quad (6)$$

Where; Y- represents EC values in mS/cm

And X- represents the reflectance values observed in satellite images given by the bands combination 'B1 + B2 + B3 + B8' (dos Santos, 2022; Pizani *et al.,* 2020).

where;

B1- Aerosols Band of Sentinel-2 (S2A) satellite whose wavelength is 443.9nm, B2- Blue band of Sentinel-2 (S2A) satellite whose wavelength is 496.6nm, B3- green band of Sentinel-2 (S2A) satellite whose wavelength is 560nm, B8- Near Infrared Band (NIR) of Sentinel-2 (S2A) satellite whose wavelength is 835.1nm

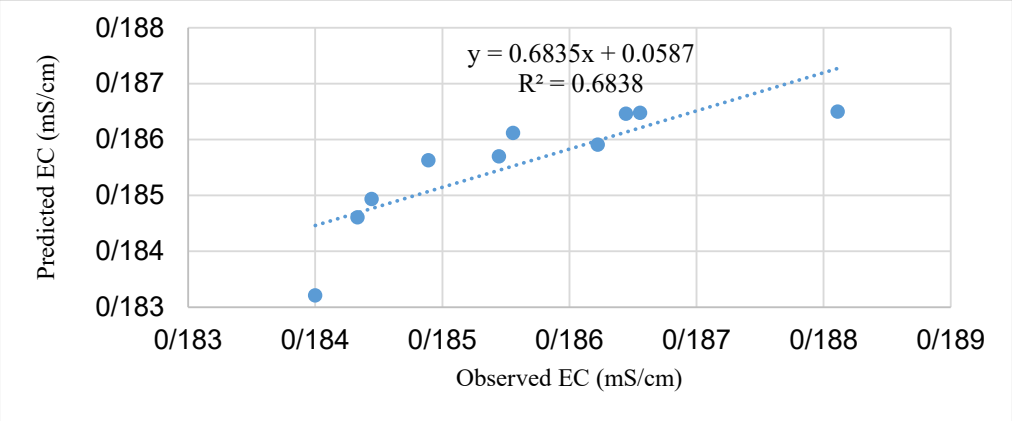

Fig 12. A scatter plot showing the linear relationship between observed and predicted EC (mS/cm) at Mindu Reservoir, November 2024–April 2025, with $R^2 = 0.6838$.

Table 10. A table of Mean observed and predicted values of water EC in the sampled locations

Pixel	Longitude (E)	Latitude (S)	In-situ measurement (M_i)- EC (mS/cm)	Predicted (P_i)- EC (mS/cm)	RMSE	MAE
1	37.61433°	6.85741°	0.18544	0.185701		
2	37.61408°	6.85745°	0.18656	0.186477		
3	37.61378°	6.85746°	0.18489	0.185629		
4	37.62065°	6.87082°	0.18644	0.186464		
5	37.61632°	6.86770°	0.18811	0.186502	0.000675	0.000512
6	37.61287°	6.86488°	0.18556	0.186118		
7	37.61043°	6.86300°	0.18622	0.185910		
8	37.60667°	6.87332°	0.18400	0.183214		
9	37.60808°	6.87494°	0.18433	0.184608		
10	37.60880°	6.87557°	0.18444	0.184935		

The regression analysis as shown in Table 11 below, between the observed and predicted water EC demonstrates a p-value of 0.003 which is lower than the critical value of 0.05, meaning that the results are statistically significant and there is only 0.3% that the observed correlation between the observed and predicted water EC is due to chance. Therefore, the null hypothesis stating "**there is no correlation between observed and predicted water EC values**" is rejected.

Table 11. A table of regression analysis for water EC concentration

ANOVA					
	df	SS	MS	F	p-value
water EC Regression	1	6.7E-06	6.7E-06	17.29703	0.00317
Residual Error	8	3.1E-06	3.88E-07		
Total water EC Variation	9	9.8E-06			

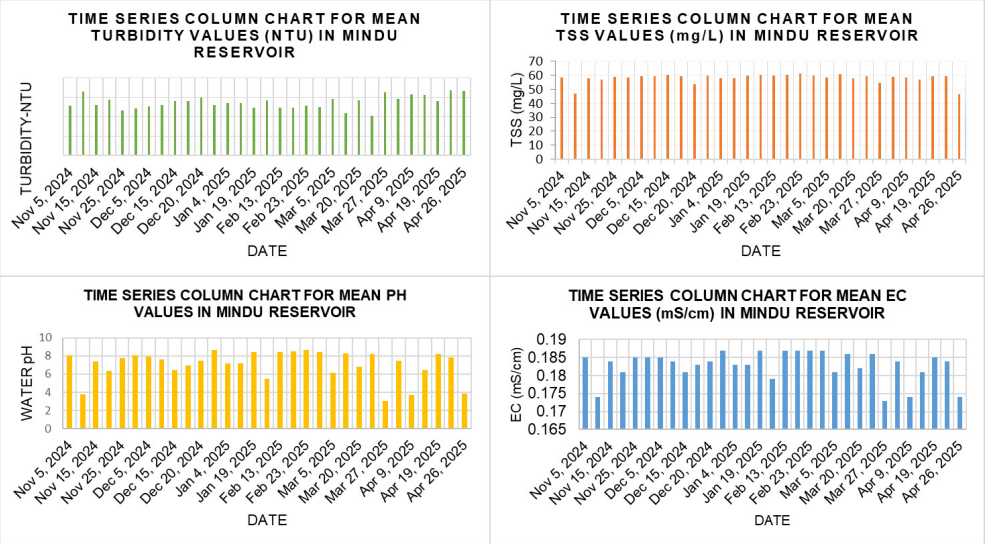

Fig 13. Column charts of time series variation of water quality parameters in the Mindu Reservoir, November 2024–April 2025

Table 12. A summary table of observed (in-situ) Spatial statistical values

PARAMETER	DATE	SAMPLING POINTS	MINIMUM OBSERVED	MAXIMUM OBSERVED	MEAN	STANDARD DEVIATION
TSS	Nov-2024	6	10	100	27.04	18.33
PH	to Apr-2025	10	6.5	10.13	8.158	0.674485393
EC		10	0.118	0.257	0.187482	0.0282
TURBIDITY		10	21.4	97	55.6945	18.7886

Accuracy assessment

Figure 8,9,10, and 11affirm the strength of the regression models by showing correlation with high coefficient of determination (R^2) between predicted values and observed data. Using the pre-stated equations of R^2, RMSE, and MAE, the accuracy of the algorithms and predicted values was checked and summarized in Table 13 below

Table 13. A table of Algorithms, R2, RMSE, and MAE

ARAMETER	Algorithm	R^2	RMSE	MAE
TSS	0.8046x + 5.5561	0.8046	2.2484	2.0160
PH	0.7394x + 2.1609	0.7394	0.0857	0.0647
EC	0.6835x + 0.0587	0.6838	0.000675	0.000512
URBIDITY	0.7214x + 16.255	0.7214	2.0440	1.8450

Table 14. Classification of coefficient of determination (R2) values (Nikoo et al., 2024).

Performance rating	R^2
Very good	$R^2 \geq 0.7$
Good	$0.5 \leq R^2 < 0.7$
Satisfactory	$0.3 \leq R^2 < 0.5$
Unsatisfactory	$R^2 < 0.3$

Table 15. Limit for irrigation and drinking water quality related parameters by WHO (Banderi et al., 2012; ****Abbas, 2013; ***Hellar-Kihampa and Ndunguru, 2021, * Ministry of Environment, 1999).**

Parameter	Symbol	unit	Allowable range for irrigation	Maximum allowable range for drinking
Total Suspended Solids	TSS	mg/L	45*	No guideline***
Turbidity	-	NTU	-	<5***
potential of Hydrogen	pH	-	6.0-8.5**	7.0-8.5**
Electrical Conductivity	EC	mS/cm	0-3**	<1.5****

These algorithms were then featured-in the GEE–JavaScript for estimation of water quality parameters (Turbidity, TSS, EC and pH) in the Mindu Reservoir from November-2024 to April-2025 and produced water parameters' concentration maps as given in Figure 14 below

DISCUSSION

Turbidity

This study has observed a very good correlation as classified in Table 14, between in-situ water Turbidity and the reflectance values observed in satellite images over Mindu Reservoir with the Coefficient of Determination (R^2) value of 0.7214 as shown in Figure 9, which is almost similar to a study by Kapalanga et al., (2021) which had R^2 of 0.767 between predicted and measured Turbidity (NTU) values. This level of correlation indicates that approximately 72.14% of variance in water Turbidity in the Mindu Reservoir can be explained by satellite derived spectral information, indicating potentiality of Remote Sensing in retrieving water Turbidity

Water Turbidity is caused by clay, silt, CDOM, algae, plankton, inorganic and organic matters; it is scientifically proven that studies undertaken at low turbid water achieves higher R^2 values as a result of minimized interference caused by water constituents to visible radiations as an example of a study by Katlane et al., (2024), which achieved better agreement with R^2 value of 0.88 between satellite-derived Turbidity values and in-situ measurements. the observed R^2 value of 0.7214 in our study suggests presence of multiple constituents causing water Turbidity

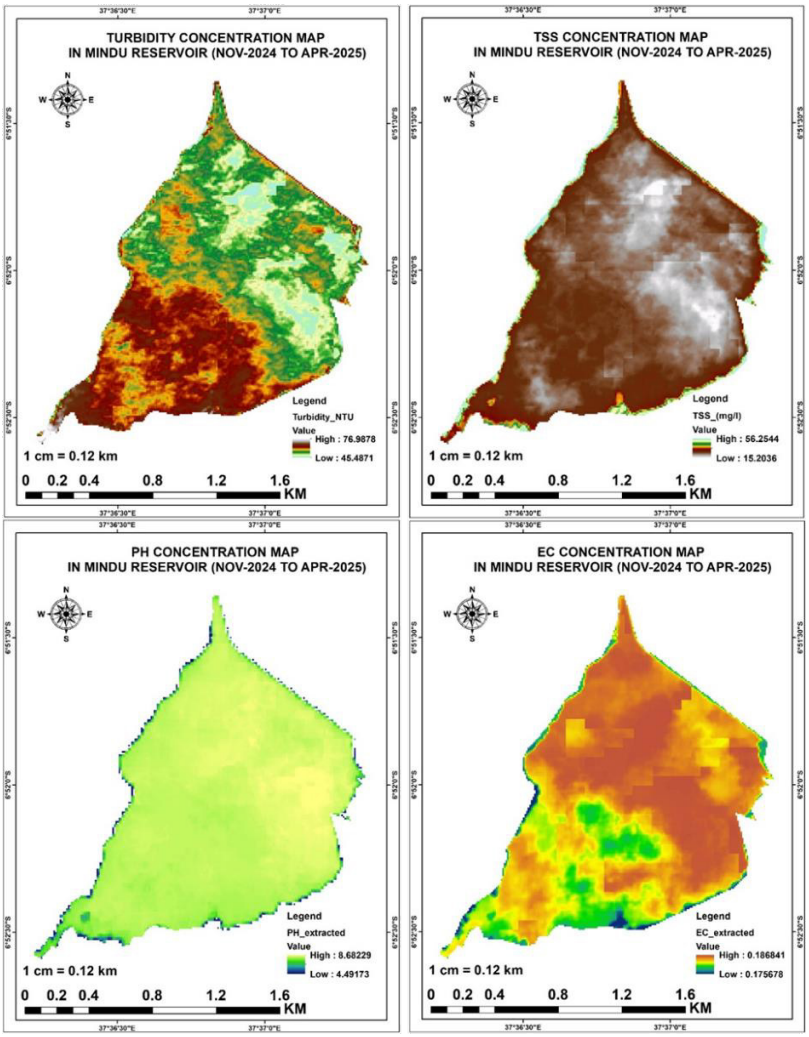

Fig 14. Concentration maps of Water parameter parameters in the Mindu Reservoir, November 2024–April2025

in Mindu Reservoir that increases scattering effect of visible radiations and reduce correlation strength (Cui et al., 2022). These constituents may be resulted from sediment input, biological activities and human activities

The general trend for water Turbidity was increasing from November-2024 to April-2025, as given in Figure 13. This may signify increasing sedimentation and water clarity with time, which may be linked to anthropogenic activities and changes in land use/cover in the catchment.

From the spatial distribution maps given in Figure 14, water Turbidity in the inlet zone of the Mindu Reservoir was observed to be highly concentrated reaching to 76.99 NTU and decreased as going to the mid-section; this signifies possibility of having soil loss from the catchment. These observed Turbidity

values are very high as compared to standards given in Table 15, which require them to be below 5 NTU for treated drinking water and below 25 NTU for natural potable water like that of Mindu Reservoir

TSS

Very good correlation has been observed between in-situ water TSS and the reflectance values observed in satellite images over Mindu Reservoir with the Coefficient of Determination (R^2) value of 0.8046 as given in Figure 10. These findings are almost similar to that of Hidayah, (2024) which had R^2 of 0.85 between in-situ water TSS and the satellite-derived TSS values. This level of correlation indicates that approximately 80.46% of variance in water TSS in the Mindu Reservoir can be explained by satellite derived spectral information, highlighting the effectiveness of remote sensing for TSS monitoring

Almost constant variation was observed from November-2024 to April-2025 with the lowest Reservoir's TSS concentration of 46.475 mg/L and the highest TSS concentration of 61.489 mg/L. However, these are very high values as compared to standards given in Table 15, which require them to be below 45 mg/L for irrigation water

In the spatial distribution maps shown in Figure 14, higher TSS values reaching 56.25 mg/L were observed in the inlet zone of the Mindu Reservoir, signifying possibility of having soil loss from the catchment

pH

This study has observed very good correlation between in-situ water pH and the reflectance values observed in satellite images over Mindu Reservoir with the Coefficient of Determination (R^2) value of 0.7394 as shown in Figure 11, however, a study by (Pizani et al., 2020) observed slightly better correlation with R^2 of 0.89 between predicted and measured water-pH values. This may be caused by site-specific environmental conditions like water Turbidity, dissolved organic matters which can influence relationship between satellite derived and in-situ measured values. The pH is related with the amount of chlorophyll and tend to increase with the presence of algaes and cyanobacteria (Pizani et al., 2020).

The general trend for water pH was decreasing from November-2024 to April-2025, as given in Figure 13, But also, higher pH values are related to greater EC values, this finding agrees with the study by (Pizani et al., 2020)

EC

This study has observed good correlation between in-situ water EC and the reflectance values observed in

satellite images over Mindu Reservoir with the Coefficient of Determination (R^2) value of 0.6838 as shown in Figure 12, which is almost similar a study by (Pizani et al., 2020) which had R^2 of 0.69 between predicted and measured water-EC values.

The general trend for water EC was decreasing from November-2024 to April-2025, as given in Figure 13, But also, higher EC values are related to greater pH values, agreeing with the findings by (Pizani et al., 2020)

In the spatial distribution as shown in Figure 14, water in the outlet section of the Mindu Reservoir was observed to have higher EC concentration reaching to 0.18684 mS/cm. These values are within allowable range for irrigation water but a bit higher than the required standards for drinking water as shown in Table 15

Limitations

The spatial resolution of sentinel-2 satellite is 10m for visible bands, 20m for SWIR and Red-Edge bands, and 60m for Aerosols as indicated in Table 3, Which may not capture all of the variations in water quality, and not able to capture variations in smaller water bodies less than 10m square. The satellite temporal resolution is five (5) days therefore; it cannot provide real-time data in the four (4) days between its successive visits, such that a new data is only obtained after the satellite has passed (five days), and thus it can also not provide future data. This study was conducted from November-2024 to April-2025 partly covering wet and dry season, therefore it may not represent long-term variations.

Conclusion

In this research, remote sensing has proved to have strong agreement with in-situ measured values for the studied water quality parameters with coefficient of determination (R2) values to be 0.7214, 0.8046, 0.7394, and 0.6838 for the Turbidity, TSS, pH, and EC respectively. The RMSE and MAE values of zero indicate a perfect fit, and values lower than half of the standard deviation of observed values can be considered to indicate a poor fit (Barraza-Moraga et al., 2022). As observed from Table 12 and 13. For all of the developed algorithms, the RMSE or MAE are higher than half of the standard deviation of observed values, indicating strong agreement of the predicted outcomes by the developed statistical models.

This study has demonstrated the applicability of Remote Sensing to monitor water quality parameters, and predict even for un-sampled locations, this makes it to be useful even in synoptic spatial and temporal coverage

of large areas, accessibility to remote and inaccessible areas, and access to historical data as the Sentinel-2 L2A imagery dataset is available since March-2017 to date. Through the created models, users can estimate water quality parameters particularly Turbidity, Electrical Conductivity (EC), potential of Hydrogen (pH) and Total Suspended Solids (TSS) and have informed decision making. This facilitates the 2030 agenda by enhancing the SDG-6 which highlights the need for protection, restoration, and sustainable management of water-related ecosystems

The developed algorithms can be used to estimate the studied water quality parameters in the Mindu Reservoir and other water bodies, since Mindu Reservoir served just as a case study in this research. However, in case they are used for other water bodies, it will be necessary for verifying their accuracy by analyzing water samples and comparing the results. This study is recommending use of the created algorithms in developing a dynamic web-application for the next studies, enhancing continuous monitoring of WQPs, as well as use of machine learning techniques to enhance real-time data accessibility and future prediction of the WQPs. This study would also like to recommend an addition of more water quality parameters (Sodium Adsorption Ratio, TDS, and Heavy Metals) and extension of the study period for the next researchers so as to capture seasonal and inter-annual water quality variations

Nomenclature

TSS- Total Suspended Solids
pH- potential of Hydrogen
EC- Electrical Conductivity
CDOM- Colored Dissolved Organic Matter
TDS- Total Dissolved Solids
MSI- Multi-Spectral Instrument
SWIR- Short Wave Infrared
SDGs- Sustainable Development Goals
WQPs- water quality parameters
GEE- Google Earth Engine
API- Application Programming Interface
BOA- Bottom of Atmosphere
GIS- Geographic Information System
GPS- Global Positioning System
RMSE- Root Mean Square Error
MAE- Mean Absolute Error
NTU- Nephelometric Turbidity Unit
MNDWI- Modified Normalized Difference Water Index
ANOVA- Analysis of Variance

References

Abbas, J. (2013). Assessment of water quality in Tigris River-Iraq by using GIS mapping. *Natural*

Resources, 2013. http://doi.org/10.4236/nr.2013.46054

Ahuja, S. (Ed.). (2021). *Handbook of water purity and quality*. Academic press.

Al Yousif, M. A., and Chabuk, A. (2023). Assessment water quality indices of surface water for drinking and irrigation applications–A comparison review. *Journal of Ecological Engineering*, *24*(5), 40-55. https://doi.org/10.12911/22998993/161194

Banderi, A., Mohammad, M. S., Hamdi, H., Shomeli, M., and Ali, S. D. (2012). Water quality assessment of Amir Kabir sugarcane agro-industry with respect to agricultural and drinking views. *Journal of Environmental Ecology, 3*(1), 11-28. http://doi.org/10.5296/jee.v3i1.2353

Barraza-Moraga, F., Alcayaga, H., Pizarro, A., Félez-Bernal, J., & Urrutia, R. (2022). Estimation of chlorophyll-a concentrations in Lanalhue Lake using Sentinel-2 MSI satellite images. *Remote Sensing*, *14*(22), 5647. https://doi.org/10.3390/rs14225647

Biswas, A., Sarkar, S., Das, S., Dutta, S., Choudhury, M. R., Giri, A., ... & Paul, D. (2025). Water scarcity: A global hindrance to sustainable development and agricultural production–A critical review of the impacts and adaptation strategies. *Cambridge Prisms: Water, 3*, e4. https://doi.org/10.1017/wat.2024.16

Chapman, D. V. (2021). *Water quality assessments: a guide to the use of biota, sediments and water in environmental monitoring*. CRC Press.

Chidiac, S., El Najjar, P., Ouaini, N., El Rayess, Y., & El Azzi, D. (2023). A comprehensive review of water quality indices (WQIs): history, models, attempts and perspectives. *Reviews in Environmental Science and Bio/Technology*, *22*(2), 349-395. https://doi.org/10.1007/s11157-023-09650-7

Cui, M., Sun, Y., Huang, C., & Li, M. (2022). Water turbidity retrieval based on UAV hyperspectral remote sensing. *Water*, *14*(1), 128. https://doi.org/10.3390/w14010128

Das, S., Nandi, D., Thakur, R. R., Bera, D. K., Behera, D., Đurin, B., & Cetl, V. (2024). A novel approach for ex situ water quality monitoring using the Google Earth engine and spectral indices in Chilika

Lake, Odisha, India. *ISPRS International Journal of Geo-Information*, *13*(11), 381.https://doi.org/10.3390/ijgi13110381

Department of Water Affairs and Forestry. (2000). Quality of Domestic Water Supplies, Volume 2: Sampling Guide.

Dogliotti, A. I., Ruddick, K. G., Nechad, B., Doxaran, D., & Knaeps, E. (2015). A single algorithm to retrieve turbidity from remotely-sensed data in all coastal and estuarine waters. *Remote sensing of environment*, *156*, 157-168. https://doi.org/10.1016/j.rse.2014.09.020

dos Santos, R. I. M. (2022). *Estimating sea surface salinity using Sentinel-2 satellite imagery* (Master›s thesis, Universidade do Porto (Portugal)).

Eslamian, S. (2016). Urban water reuse. *Nova Yorque: CRC Press Taylor & Francis Group*.

Field, A. (2024). *Discovering statistics using IBM SPSS statistics*. Sage publications limited.

Gobry, J. J., Twisa, S. S., Ngassapa, F., and Kilulya, K. F. (2023). Impact of land-use/cover change on water quality in the Mindu Dam drainage, Tanzania. *Water Practice and Technology, 18*(5), 1086-1098. https://doi.org/10.2166/wpt.2023.067

Govedarica, M., & Jakovljević, G. (2019, June). Monitoring spatial and temporal variation of water quality parameters using time series of open multispectral data. In *Seventh international conference on remote sensing and geoinformation of the environment (RSCy2019)* (Vol. 11174, pp. 298-307). SPIE. https://doi.org/10.1117/12.2533708

Hellar-Kihampa, H., & Ndunguru, P. I. (2021). Physicochemical and bacteriological water quality parameters in relation to land-use practices at a rural catchment, Mbinga District, Tanzania. *Tanzania Journal of Science*, *47*(3), 35. https://doi.org/10.4314/tjs.v47i3.35

Hidayah, Z. (2020). Estimation of total suspended solids in the Ujung Pangkah Estuary using multi-temporal Sentinel-2 satellite imagery. *ILMU DAN TEKNOLOGI KELAUTAN TROPIS Издательство: INDONESIAN OCEANOLOGISTS ASSOC BOGOR AGRICULTURAL*

UNIV, DEPT MAR SCI & TEC, JL. RAYA DARMAGA KAMPUS IPB DARMAGA BOGOR, BOGOR, INDONESIA, WEST JAVA, 16680. https://doi.org/10.29244/jitkt.v16i3.53244

Kapalanga, T. S., Hoko, Z., Gumindoga, W., & Chikwiramakomo, L. (2021). Remote-sensing-based algorithms for water quality monitoring in Olushandja Dam, north-central Namibia. *Water Supply*, *21*(5), 1878-1894. https://doi.org/10.2166/ws.2020.290

Katlane, R., Doxaran, D., ElKilani, B., & Trabelsi, C. (2024). Remote sensing of turbidity in optically shallow waters using sentinel-2 MSI and PRISMA satellite data. *PFG–Journal of Photogrammetry, Remote Sensing and Geoinformation Science*, *92*(4), 431-447. https://doi.org/10.1007/s41064-023-00257-9

Kc, A., Chalise, A., Parajuli, D., Dhital, N., Shrestha, S., & Kandel, T. (2019). Surface water quality assessment using remote sensing, GIS and artificial intelligence. *Technical Journal*, *1*(1), 113-122. https://doi.org/10.3126/tj.v1i1.27709

Kimambo, O. N., Chikoore, H., Gumbo, J. R., & Msagati, T. A. (2019). Retrospective analysis of Chlorophyll-a and its correlation with climate and hydrological variations in Mindu Dam, Morogoro, Tanzania. *Heliyon*, *5*(11). https://doi.org/10.1016/j.heliyon.2019.e02834

Koncagül, E., Tran, M., & Connor, R. (2020). The United Nations world water development report 2020: Water and climate change, facts and figures.

Lu, M., Li, F., Zhan, B., Li, H., Yang, X., Lu, X., & Xiao, H. (2020). An improved cloud detection method for GF-4 imagery. *Remote Sensing*, *12*(9), 1525. https://doi.org/10.3390/rs12091525

Machiwa, P. K. (2003). Water quality management and sustainability: the experience of Lake Victoria Environmental Management Project (LVEMP)—Tanzania. *Physics and Chemistry of the Earth, Parts A/B/C*, *28*(20-27), 1111-1115. https://doi.org/10.1016/j.pce.2003.08.032

Markandya, A. (2006). Water quality issues in developing countries. *Economic development and environmental*

sustainability: New policy options, 307-344.

Ministry of Environment, Human Resource Development and Employment, Department of Environment. (1999). Guidelines for irrigation water quality (General Notice No. 617 of 1999). Government of Tanzania.

Ngonyani, Consolatha J. & Nkotagu, H. H. (2007). Study of nutrient pollutants and their impacts on the water quality of the Mindu reservoir at Morogoro Municipality. *Tanzania Journal of Engineering and Technology*, *1*(3), 138-148.

Nikoo, M. R., Zamani, M. G., Zadeh, M. M., Al-Rawas, G., Al-Wardy, M., & Gandomi, A. H. (2024). Mapping reservoir water quality from Sentinel-2 satellite data based on a new approach of weighted averaging: Application of Bayesian maximum entropy. *Scientific Reports*, *14*(1), 16438. https://doi.org/10.1038/s41598-024-66699-2

Pauw, K., & Thurlow, J. (2011). Agricultural growth, poverty, and nutrition in Tanzania. *Food policy*, *36*(6), 795-804. https://doi.org/10.1016/j.foodpol.2011.09.002

Pizani, F. M., Maillard, P., Ferreira, A. F., & de Amorim, C. C. (2020). Estimation of water quality in a reservoir from Sentinel-2 MSI and Landsat-8 OLI sensors. *ISPRS Annals of the Photogrammetry, Remote Sensing and Spatial Information Sciences*, *3*, 401-408. https://doi.org/10.5194/isprs-annals-V-3-2020-401-2020

Sankaran, R., Al-Khayat, J. A., Chatting, M. E., Sadooni, F. N., & Al-Kuwari, H. A. S. (2023). Retrieval of suspended sediment concentration (SSC) in the Arabian Gulf water of arid region by Sentinel-2 data. *Science of the Total Environment*, *904*, 166875. https://doi.org/10.1016/j.scitotenv.2023.166875

Sweetnam, C. (2004). Water quality sampling procedures.

World Water Quality Alliance. (2021). World water quality assessment: First global display of a water quality baseline. *A consortium effort by the world water quality alliance—Towards a full global assessment. Information document annex for display at the 5th session of the united nations environment assembly, Nairobi 2021*.

Zhang, X., Huang, J., Chen, J., & Zhao, Y. (2023). Remote sensing monitoring of total suspended solids concentration in Jiaozhou Bay based on multi-source data. *Ecological Indicators*, *154*, 110513.https://doi.org/10.1016/j.ecolind.2023.110513